Supplemental Data

Supplemental Figure Legends

Figure S1 (related to Figure 1): Focal adhesion complexes in the wandering 3rd instar ED and OS.
Labeling of the focal adhesion complex components in the wandering 3rd instar (wL3) eye disc and OS. All glial membranes were labeled using repo-GAL4>CD8::GFP (A,B: green); repo-GAL4>CD8::RFP (E,F: blue). Neurons were immunolabeled using anti-HRP (A,B: blue) and nuclei using DAPI (C,D: blue). βPS integrin was detected through immunolabeling (A-I; red) and the alpha integrin subunits were labeled using αPS2 endogenously tagged with YFP (αPS2::YFP, C,D: green) and immunolabeling for αPS3 (H,I: blue). Other focal adhesion components were labeled using Talin and Integrin linked kinase (ILK) endogenously tagged with GFP (Talin::GFP, E-G: green)(ILK::GFP, H,I: green).
All panels are single 0.2 μm Z-sections and for all panels single Z sections at the basal side (basal) and through the mid point (mid) are shown. Dashed lines show where the cross sections (B, D, G, I) are obtained. White boxed regions were shown in higher magnification in small panels (F). In all tissues, focal adhesion complexes including integrins, Talin and ILK were seen throughout the OS and ED. Note that the complexes were strongly detected at the basal level of the OS where glia contact the neural lamella. Scale bars are 10 μm.

Figure S2 (related to Figure 2): Knock down of integrin and OS morphological changes in the early 3rd instar.
repo-GAL4 was used to express βPS-RNAi and talin-RNAi in all glia. UAS-CD8::GFP (green) labeled glial membranes and DAPI (blue, A-C) marked nuclei. Images were projections of 0.2 μm Z-stacks. In controls (A and D), βPS (red) and αPS3 (blue, D) immunolabeling was detected as puncta in the eye disc and OS. These puncta were absent in βPS-RNAi treated OS (B) and decreased in talin-RNAi OS (C and E) (arrows), but still present in the eye disc epithelia (double arrows). Similarly immunolabeling for Talin was observed in puncta (F, red) throughout the wild-type OS labeled with NrxIV::GFP (green) and was reduced in the OS (G, arrow) of Talin-RNAi but retained in the ED (G, double arrow) and the photoreceptor axons. Note that the PG were concentrated in the anterior half (close to ED) and reduced in the posterior half (arrowheads) of RNAi OS. Scale bars are 5 microns (A-F) and 10 microns (G).

Figure S3 (related to Figure 3): Dye penetration after βPS, talin and NrxIV knockdown in OS and peripheral nerves.
Dye permeability assays were conducted to determine the degree of blood-nerve-barrier disruption with loss of integrin and talin in the glia. In control animals, Alexa-647 conjugated dextran was excluded from the interior of the peripheral nerve (A) and the OS (E). The penetration of the fluorescent dye significantly increased in the peripheral nerve (B-D) and OS (F-H) when NrxIV-RNAi (positive control), βPS-RNAi or talin-RNAi were expressed in either the subperineurial (SGP-GAL4) or all glia (repo-GAL4). The quantification of the dye penetration into the OS for βPS-, talin- and NrxIV-RNAi is

shown in Figure 3.

Figure S4 (related to Figure 4): Photoreceptor axon targeting defects in RNAi adults.
A monoclonal 24B10 antibody was used to label photoreceptor axon in adult fly eye-brain complexes. In controls (A), 24B10 labeled photoreceptor axons terminated properly in the optic lobe (OL). Note that left panel shows axonal termination in both lamina (La) and medulla (Me) layers and only medulla was preserved in the right panel. In RNAi flies (B,C), different neuronal defects were observed, which included disorganized axons termination (arrowheads) and lack of photoreceptor innervation (B, C) in the optic lobe. Smaller optic lobes were seen associated with the abbreviated axonal termination. Dashed lines show the boundary between the optic lobe and midbrain (MB).

Figure S5 (related to Figure 5): Axon stalling phenotypes
Examples of axonal stalling and associated glia in the OS (C-E) or ED (A,B,B'). The stalling region was shown by single optic sections either from the middle of the Z-stack (mid) or from the basal level (basal). Regions in white boxes are digitally magnified and displayed in the right panels. Arrows point to the glia associated with the stalled axon terminals.
C-E) Partial stalling phenotypes were observed (C,D) and these represented relatively rare cases where only subsets of photoreceptor axons (arrows) were stalled in the RNAi OS while others migrated through. E) An example of axonal stalling (arrow) at the boundary of the ED and OS.
All panels are single 0.2 μm Z-sections. Scale bars are 10 μm.

Figure S1

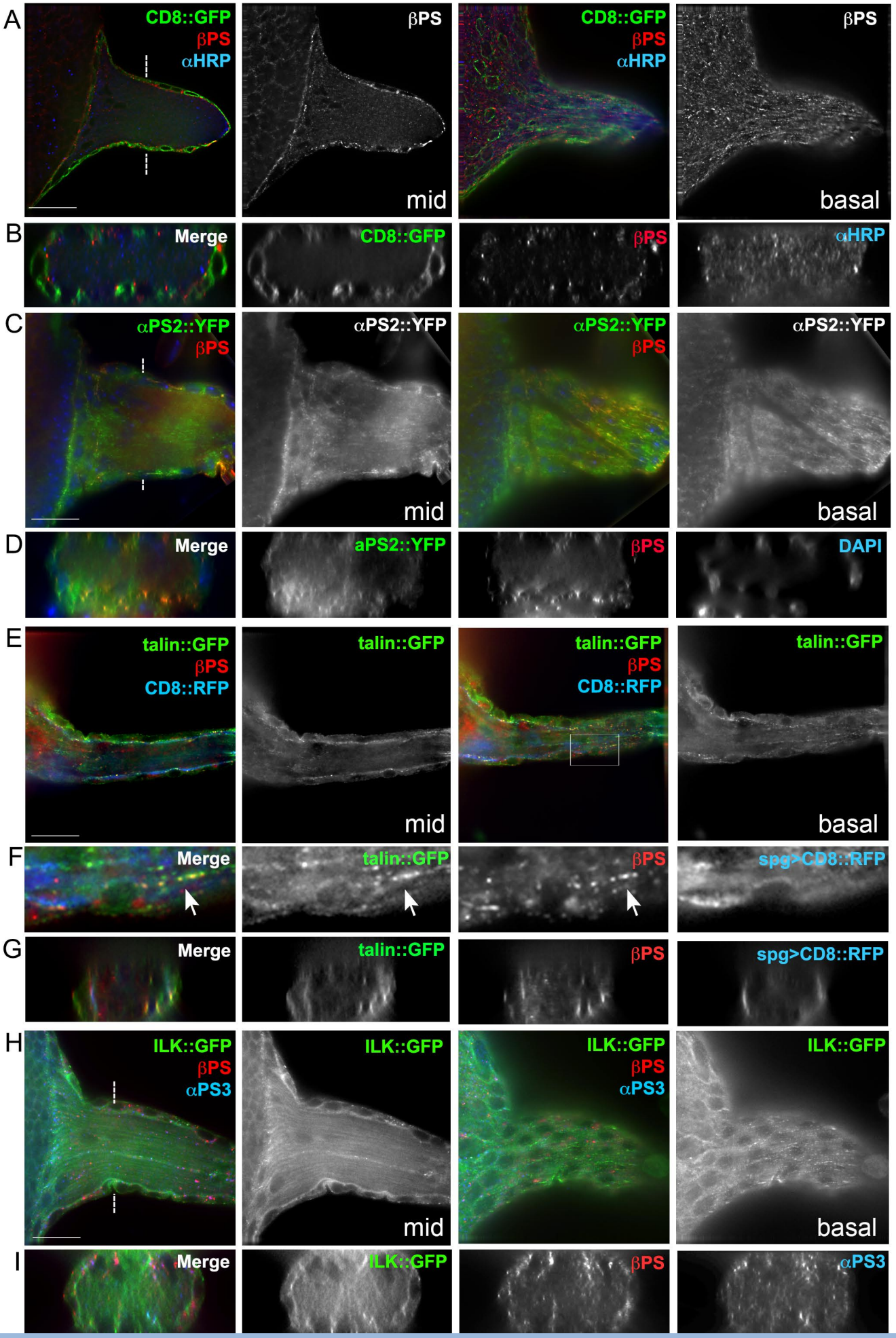
A
CD8::GFP
βPS
αHRP
βPS
mid
CD8::GFP
βPS
αHRP
βPS
basal
B
Merge
CD8::GFP
βPS
αHRP
C
αPS2::YFP
βPS
αPS2::YFP
mid
αPS2::YFP
βPS
αPS2::YFP
basal
D
Merge
aPS2::YFP
βPS
DAPI
E
talin::GFP
βPS
CD8::RFP
talin::GFP
mid
talin::GFP
βPS
CD8::RFP
talin::GFP
basal
F
Merge
talin::GFP
βPS
spg>CD8::RFP
G
Merge
talin::GFP
βPS
spg>CD8::RFP
H
ILK::GFP
βPS
αPS3
ILK::GFP
mid
ILK::GFP
βPS
αPS3
ILK::GFP
basal
I
Merge
ILK::GFP
βPS
αPS3

Figure S2

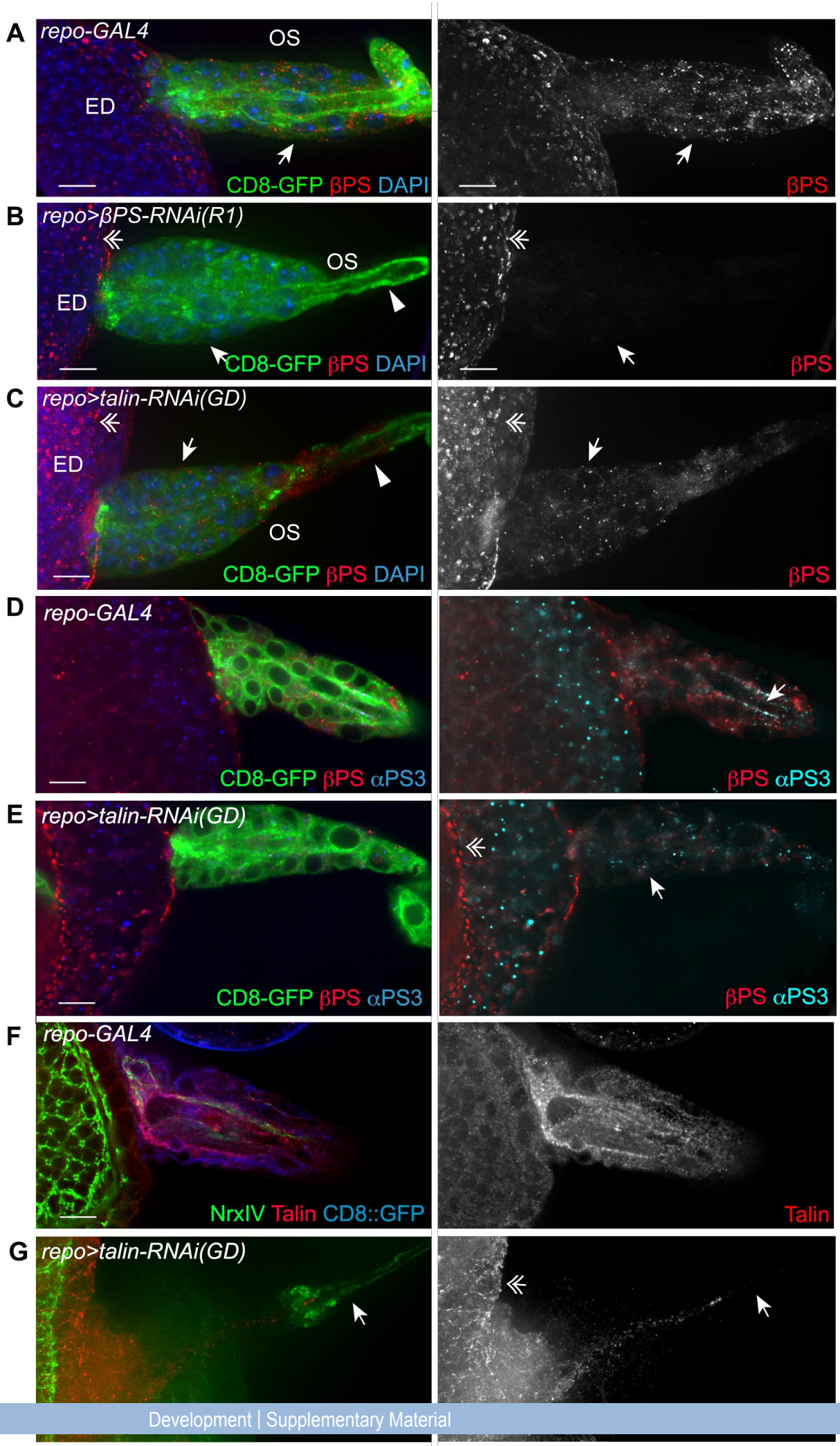
A
repo-GAL4
OS
ED
CD8-GFP βPS DAPI
βPS
B
repo>βPS-RNAi(R1)
OS
ED
CD8-GFP βPS DAPI
βPS
C
repo>talin-RNAi(GD)
ED
OS
CD8-GFP βPS DAPI
βPS
D
repo-GAL4
CD8-GFP βPS αPS3
βPS αPS3
E
repo>talin-RNAi(GD)
CD8-GFP βPS αPS3
βPS αPS3
F
repo-GAL4
NrxIV Talin CD8::GFP
Talin
G
repo>talin-RNAi(GD)

Figure S3

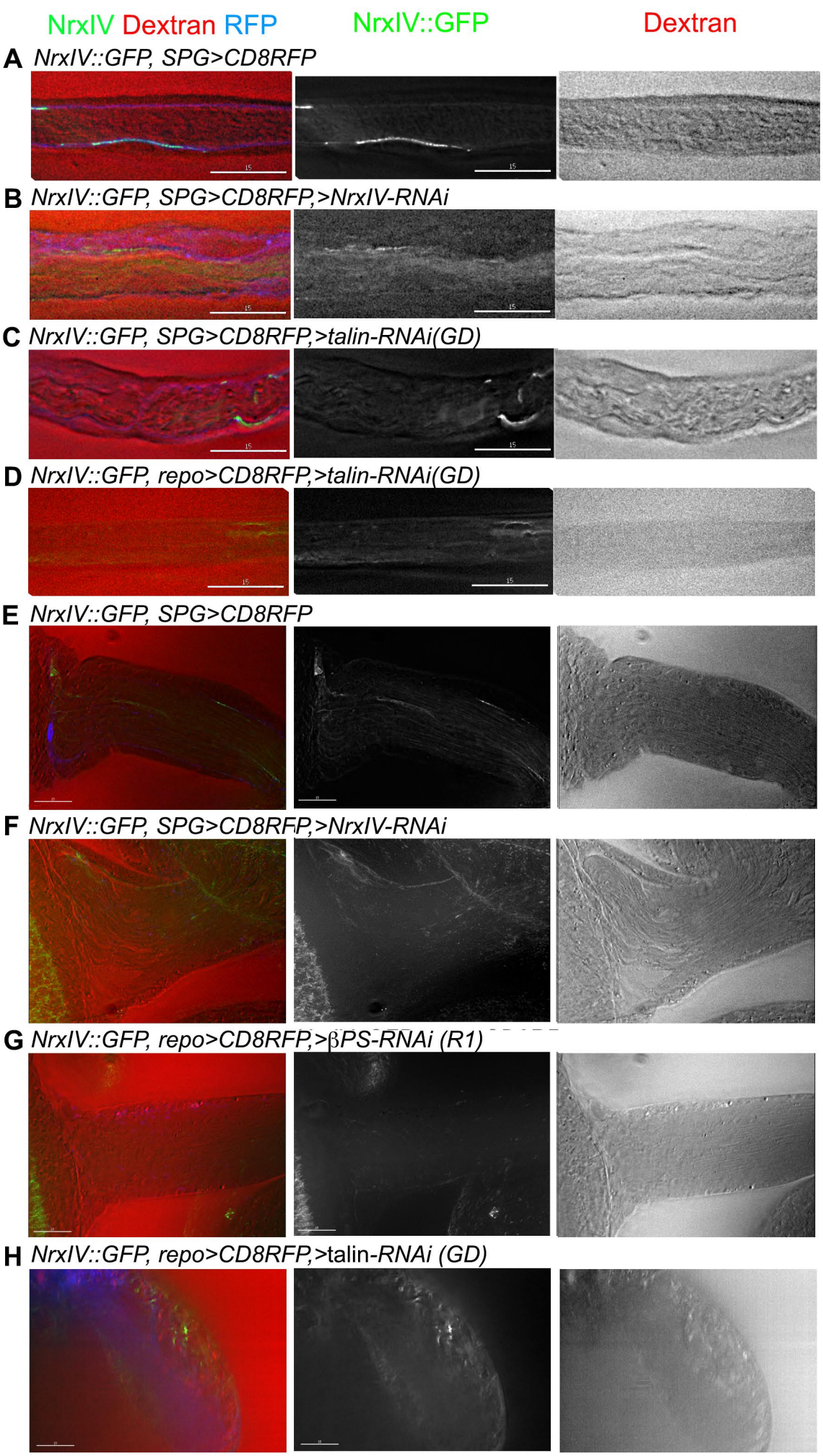
NrxIV Dextran RFP
NrxIV::GFP
Dextran
A NrxIV::GFP, SPG>CD8RFP
B NrxIV::GFP, SPG>CD8RFP,>NrxIV-RNAi
C NrxIV::GFP, SPG>CD8RFP,>talin-RNAi(GD)
D NrxIV::GFP, repo>CD8RFP,>talin-RNAi(GD)
E NrxIV::GFP, SPG>CD8RFP
F NrxIV::GFP, SPG>CD8RFP,>NrxIV-RNAi
G NrxIV::GFP, repo>CD8RFP,>βPS-RNAi (R1)
H NrxIV::GFP, repo>CD8RFP,>talin-RNAi (GD)

Figure S4

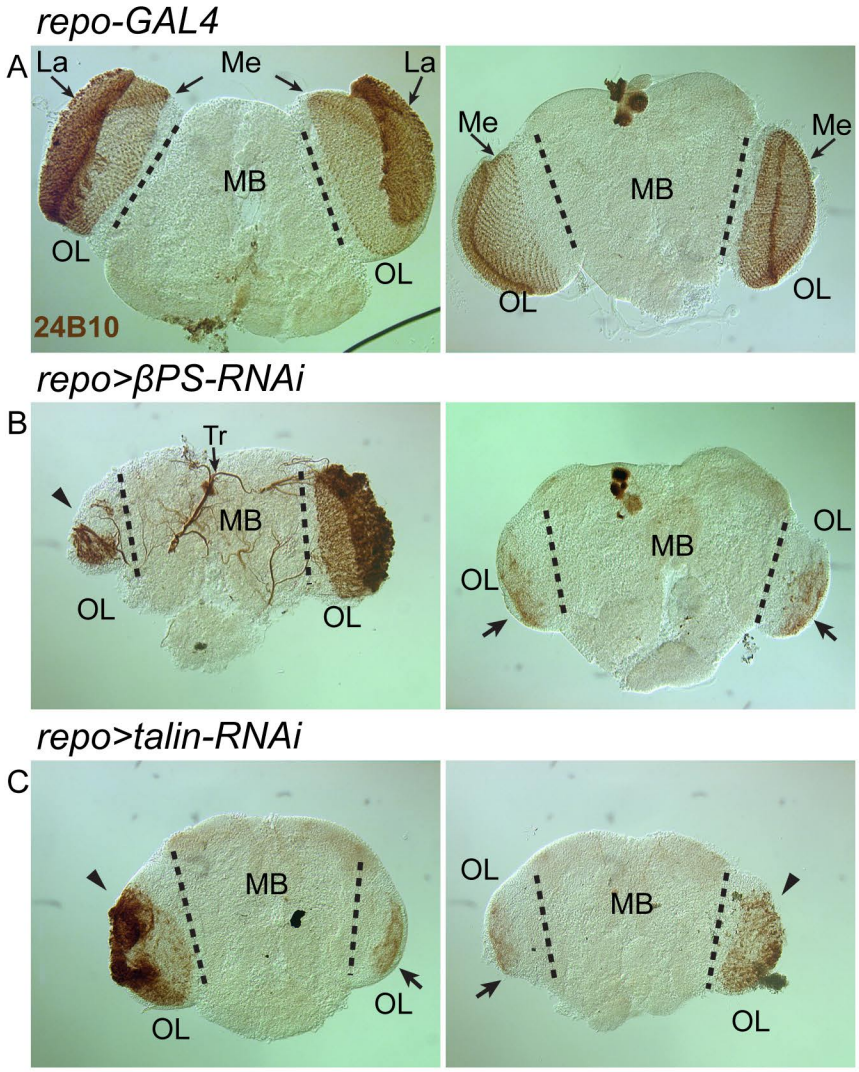
repo-GAL4
A
La
Me
La
MB
OL
OL
24B10
Me
Me
MB
OL
OL
repo>βPS-RNAi
B
Tr
MB
OL
OL
MB
OL
OL
repo>talin-RNAi
C
MB
OL
OL
OL
MB
OL

Figure S5

repo>CD8::GFP>βPS-RNAi (R1)